Desalination and Water Treatment
www.deswater.com

doi: 10.5004/dwt.2023.29662

299 (2023) 50–61
July

Preparation of lignosulfonate-based polycatecholamine composite membrane for efficient separation

Ruoyao Zhou[a], Yanxin Song[b], Tingting Gao[c], Yue Wu[a,*], Qinze Liu[a,*], Jinshui Yao[a], Changbin Zhang[d]

[a]*School of Materials Science and Engineering, Qilu University of Technology (Shandong Academy of Sciences), #3501 Daxue Road, Western University Science Park, Jinan City 250353, Shandong Province, China, Tel.: +008613173004716/+008613869145677; emails: yuewu_007@qlu.edu.cn (Y. Wu), liuqinze@qlu.edu.cn (Q. Liu), zry13173004716@163.com (R. Zhou), yaojsh@163.com (J. Yao)*
[b]*School of Chemical Engineering & Pharmacy, Jining Technician College, Jining 272100, China, email: syxlhy001@163.com (Y. Song)*
[c]*School of Chemistry and Chemical Engineering, Qilu University of Technology (Shandong Academy of Sciences), Jinan City 250353, Shandong Province, China, email: ttgao@qlu.edu.cn (T. Gao)*
[d]*Research Center for Eco-Environmental Sciences, Chinese Academy of Science, Beijing 100085, PR China, email: cbzhang@rcees.ac.cn (C. Zhang)*

Received 20 January 2023; Accepted 30 May 2023

ABSTRACT

Effective, safe, and rapid treatment of dye-contaminated wastewater is a challenging task at the global scale. In this study, lignosulfonate-based polycatecholamine and polyethersulfone composite (PES-PCA-LS) membrane was prepared by depositing aminated sodium lignosulfonate (LS) and catechol on polyethersulfone (PES) membrane. This membrane was characterized by various techniques and its performance was investigated using Congo red (CR) as the probe molecule. The results showed that the retention rate of CR solution by PES-PCA-LS membrane was above 99.5%. At this removal rate, one square meter of membrane could treat 351 L of CR waste solution (CR, 100 ppm; salt, 5,000 ppm). However, the retention rates of NaCl, Na_2SO_4, and K_2SO_4 were found to be only 2.8%, 3.5%, and 0.9%, respectively. Besides, this membrane could target selective removal of CR from the mixed solution (CR/Rhodamine B). This PES-PCA-LS membrane also showed excellent cycling performance, with the removal rate maintained at about 97% at the tenth cycle. Thus, this study provides new ideas for the application of industrial lignin in the field of membrane separation for dye/salt or dye/dye mixed solutions.

Keywords: Catechol; Lignosulfonate; Membrane; Dye; Adoption; Water treatment

1. Introduction

Color is one of the elements of nature that makes human life more aesthetic and fascinating. Dyes are widely used colored organic compounds that impart color to various substrates. However, unfortunately, textile industries generate and discharge millions of tons of highly contaminated dye-containing wastewater with diverse range of persistent pollutants during the process of preparation and utilization of dyes every year [1–3]. Most organic dyes are organic aromatic compounds with high biological toxicity and are carcinogenic, mutagenic, or teratogenic [4–8]. For example, Congo red (CR) is a drastic nuisance with many unfavorable characteristics such as high-water solubility, long-term stable existence in water bodies, non-biodegradable, and carcinogenic. Besides, high concentrations of salts (such as NaCl and Na_2SO_4) are also present in the dye-contaminated wastewater, as they are used as an adhesion promoter

* Corresponding author.

between the dyes and the fiber in the dyeing process [9–11]. Therefore, effective dyes/salt separation approaches have been a hot yet challenging research topic due to the complexity of the composition of such wastewater, nanoscale solute size, and complex interactions.

Currently, the treatment methods for dye-contaminated wastewater generally include adsorption, membrane separation, catalysis, biodegradation, and other methods [1,12–15]. Among them, membrane separation technology has been considered as the most advantageous one because of its safe operation, not requiring the addition of chemical reagents, high efficiency, and not involving any phase change [16,17]. The most used membranes in treatment of dye-contaminated wastewater are polymeric membranes, due to their cost effectiveness, high flux, controllable pore size, scalability, and flexibility in membrane formation [18,19]. For example, commercial polyethersulfone (PES) membranes offer the advantages of high stability, acid and alkali resistance, and high potential for surface modification [20]. However, inherent hydrophobicity of these membranes often leads to contamination and blockage of membrane pores, thus preventing their long-term use. Commercial PES membranes must be hydrophilic with improved adsorption performance, if they are to be used in dye separation applications [21]. To this end, significant research attempts have been made to improve the durability and hydrophilicity of polymeric membranes [11,22–24]. In recent years, the use of bio-based materials to modify polymeric membranes has become a research trend. For example, polymeric membranes were modified with dopamine to obtain excellent dye and salt separation properties and heavy metal adsorption properties [23,25]. Similarly, lignin and its derivatives are often used in the modification of polyacrylonitrile fiber membranes, endowing them with excellent hydrophilic and dye adsorption properties. [26,27]. The addition of modified material also improves the target removal performance of the membrane for dyes. This lays the foundation for separating mixed solutions of dyes and salts.

Dopamine, inspired by Mussel adhesion protein, is extensively used in surface chemistry, biomedicine, marine engineering, and household chemicals because of its excellent biocompatibility, adhesion [28–32], and ease of polymerization. The abundant –OH, –NH_2, and –NH– groups in dopamine not only facilitate secondary reactions, but also exhibit excellent chelating and electrostatic effects on heavy metal ions and dye molecules [29,33–36]. However, the high cost of dopamine limits its practical applications. Therefore, polycatecholamines (PCAs) were utilized instead of polydopamine [37–39]. For example, Zhang et al. [40] utilized tannic acid and diethylenetriamine to modify the surface of commercial membranes by co-deposition to realize hydrophilic–lipophilic translation, which could be achieved by simple water and ethanol immersion, with an oil–water separation efficiency of up to 98%.

Lignin sulfonate, a type of industrial lignin, is one of the by-products of the sulfite pulp with high yield, low cost, and environmental friendliness [41,42]. It is well known that lignin sulfonate is an underutilized biomass and therefore its exploitation has received significant research attention in recent years. The presence of phenolic hydroxyl groups offers good reactivity. The presence of sulfonyl groups, phenolic hydroxyl groups, or aromatic rings endow lignin sulfonate with excellent chelating effect on many heavy metal ions and dye molecules [43–46]. However, the water solubility limits its practical application in the field of adsorption, and thus modifications are required to obtain the desired characteristics [47]. In recent years, Gao et al. [48] obtained an adsorbent (PCA-LS) by modifying sodium lignin sulfonate (LS) with PCAs based on the Mannich reaction, which could adsorb CR at the rate of 974 $mg \cdot g^{-1}$.

In this study, commercial PES membranes were successfully modified using lignosulfonate-based polycatecholamine (PCA-LS). The surface morphology, hydrophilicity, structure, surface charge, filtration performance, and antifouling properties of the lignosulfonate-based polycatecholamine and polyethersulfone composite (PES-PCA-LS) membrane were investigated and compared with those of PES membrane. Finally, the effects of lignin addition ratio and reusability were also investigated.

2. Experimental set-up

2.1. Materials

Methyl blue (MB), Rhodamine B (RB), CR, Malachite green (MG), tetraethylenepentamine (TEPA, chemically pure, 90%), the molecular structure of the four dyes is shown in Fig. 6, LS, and formaldehyde solution (37 wt.%) were obtained from Shanghai Maclean Biochemical Technology Co., Ltd., (China). Catechol (AR) was obtained from Shanghai Aladdin Biochemical Technology Co., Ltd., (China). Hydrochloric acid (AR) was obtained from Yantai Far East Fine Chemical Co., Ltd., (China). Sodium hydroxide (AR), sodium chloride (AR), and anhydrous sodium sulfate (AR) were purchased from Chengdu Kolon Chemical Co., Ltd., (China). Anhydrous sodium sulfate (AR) was obtained from Tianjin Damao Chemical Reagent Factory (China). Anhydrous potassium sulfate (AR, >99%) was obtained from Tianjin Guangfu Technology Development Co., (China). PES membrane (0.22 μm) was obtained from Tianjin Jinteng Experiment Equipment Co., Ltd., (China).

2.2. Preparation process of PES-PCA-LS membrane

LS (1.00 g) was dissolved in ultrapure water (100 mL), which was followed by the addition of TEPA (2.10 g) and formaldehyde solution (37 wt.%, 0.81 g). When the pH was not adjusted, the pH of the mixed solution was between 10.5 and 11. The mixture was allowed to react at 90°C for 8 h. Next, this reaction solution was allowed to cool down to room temperature. Then, catechol (1.11 g) was added, PES membrane was immersed, and the contents were shaken at 30°C for 6–72 h. The PES-PCA-LS membrane, which can be stored at room temperature for long duration, was obtained by repeatedly rinsing in deionized water [40].

The molar ratio of formaldehyde, TEPA, and catechol was maintained constant at 1:1:1 during the experiment, and five products were obtained by modulating the mass ratio of LS to TEPA. The mass ratio of LS to TEPA was 0:1 (PES-PCA-LS-0), 0.25:1 (PES-PCA-LS-0.25), 0.5:1 (PES-PCA-LS-0.5), 0.75:1 (PES-PCA-LS-0.75), 1:1 (PES-PCA-LS-1), respectively.

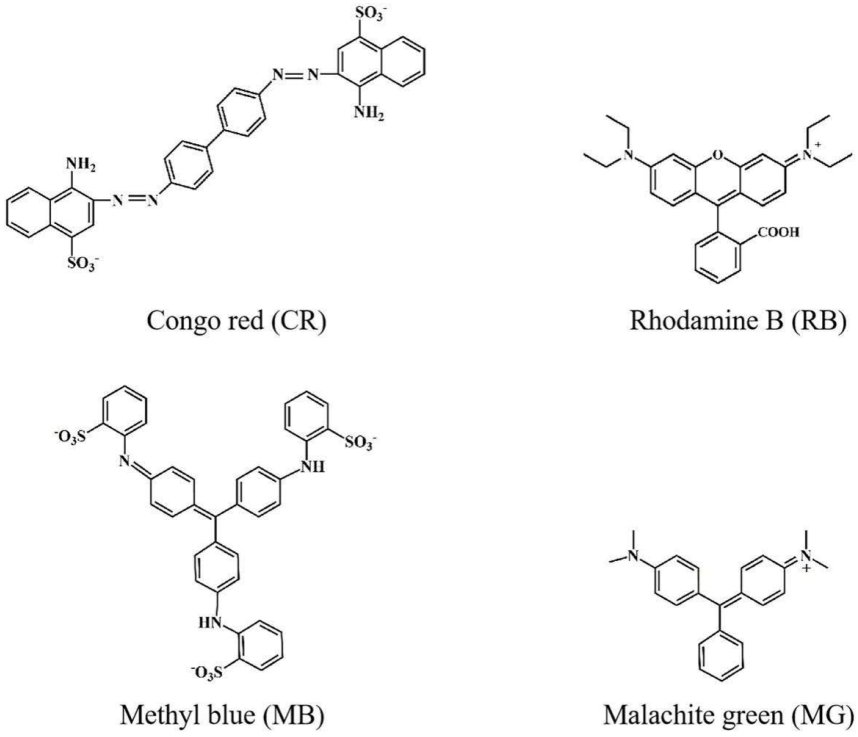

Fig. 1. Molecular formula of dyes.

The PCA-LS powder was prepared without PES membrane and the reaction time changed from 24 to 72 h. The PCA powder was prepared by directly using catechol and TEPA.

2.3. Characterization of PES-PCA-LS membrane

PCA-LS powder, PCA powder, PES membrane, and PES-PCA-LS-0.5 were scanned in the wave number range of 4,000–500 cm^{-1} by Fourier-transform infrared spectroscopy (Nicolet iS10, USA). An ultraviolet (UV) spectrophotometer (UV-2550, Shimadzu, Japan) was used to determine the dye concentration. Scanning electron microscopy (SEM, TESCAN MIRA LMS, CZ) was used to characterize the surface and cross-section morphologies of the PES and PES-PCA-LS-0.5 membranes The zeta potential of membrane was measured by solid-state zeta point analysis (GmbH-SurPASS 3, Anton Paar). The water contact angles of membrane were measured using a contact angle meter (DataPhysics-OCA20, GER). The concentrations of NaCl, Na_2SO_4, and K_2SO_4 in the solutions before and after filtration were measured by inductively coupled plasma-atomic emission spectroscopy (ICP-AES, Thermo Scientific iCAP 7400 OES, USA). The surfaces of PES and PES-PCA-LS membranes were scanned by atomic force microscopy (AFM, Germany, BRUKER, BRUKER Dimension Icon). The pore size of PES-PCA-LS-0.5 membrane and its distribution were measured by Brunauer–Emmett–Teller (BET) method (ASAP2460-Mac-US). First, the pores were degassed at 50°C for 8 h. The pore-size distribution was calculated by using the nonlocal density functional theory according to the measured N_2 adsorption–desorption isotherms at 77 K in liquid nitrogen bath.

2.4. Dye separation and antifouling ability analysis

PES-PCA-LS membrane with an effective area of 12.56 cm^2 was used to separate a mixture of CR and NaCl (pH = 6.0–6.5, 100 ppm for dye and 5,000 ppm for inorganic salts) under gravity. Each time, 10 mL of the permeate was collected and the dye concentration in the permeate was measured. The removal rate of PES-PCA-LS membrane was calculated according to the following equation [11]:

$$R = \left(1 - \frac{C_p}{C_f}\right) \times 100\% \tag{1}$$

where C_f and C_p are the concentrations of solutes in the feed and permeate, respectively.

The dye removal rate higher than 99.5% was taken as the effective removal rate, and the maximum volume of CR waste solution that could be treated per square meter was calculated as the maximum effective decontamination volume (performance). It was calculated as follows:

$$\text{Performance} = \frac{\Delta V}{A} \tag{2}$$

where performance is the maximum effective decontamination volume ($L \cdot m^{-2}$), ΔV is the permeate volume (L), and A is the effective area of the membrane under test (m^2).

The dye solution flux of PES-PCA-LS membrane was calculated as follows:

$$J = \frac{\Delta V}{A \times \Delta t} \tag{3}$$

where J is the water flux (L·m^{-2}·h^{-1}), ΔV is the volume of permeate water (L), A is the effective area of the membrane under test (m^2), and Δt is the test time (h).

Following the study to remove CR, the used PES-PCA-LS membrane was washed with alkali to desorb the adsorbed CR and the pure water flux of the regenerated membrane was measured. The CR removal test was further continued with the same membrane under the same conditions. This cycle was repeated successively to complete 10 recycle runs. Pure water flux and CR solution flux were calculated after 10 cycles. The antifouling ability of the pure PES and PES-PCA-LS membranes was investigated by using the flux recovery ratio (FRR) and flux decline ratio due to reversible (R_r) and irreversible fouling effects (R_{ir}) [49].

$$\mathrm{FRR} = \frac{J_t}{J_i} \times 100\% \tag{4}$$

$$R_r = \frac{J_t - J_{\mathrm{CR}}}{J_i} \times 100\% \tag{5}$$

$$R_{ir} = \frac{J_i - J_t}{J_i} \times 100\% \tag{6}$$

where J_i is the initial pure water flux of the unfouled fresh membrane, J_t is the pure water flux observed for the same membrane after 10 recycles, and J_{CR} denotes the permeate flux of the CR solution through the unfouled fresh membrane.

3. Results and discussion

3.1. Characterization of PES-PCA-LS membrane

LS containing many phenolic hydroxyl groups, easily undergoes electrophilic addition reaction, and attacks the carbon atoms adjacent to the phenolic hydroxyl groups during Mannich reaction with formaldehyde and TEPA. The intermediate product (TEPA-LS) was obtained after the completion of the Mannich reaction. Fig. 2 illustrates that TEPA-LS and catechol were co-deposited on PES membrane to modify its surface, and thus its separation ability was improved. Fig. 3a exhibits that the surface color is different between PES and PES-PCA-LS membranes and the latter is deeper, which was caused by the deposited PCA-LS. After filtration, the PES-PCA-LS membrane changed obviously. The color of CR is shown on the effective filtration area. Thus, the modification might have been successful. Fig. 3b exhibits the presence of a clear adsorption peak of sulfonic acid in the infrared spectra of PCA-LS compared to that of PCA, at 1,030 cm^{-1}, which confirms the successful occurrence of Mannich reaction. Compared to the peaks in the infrared spectra of PES membrane, the adsorption peaks of PCA-LS appeared for PES-PCA-LS membrane at 1,540 cm^{-1}, which confirms the successful modification.

The front surface and side section morphologies of PES and PES-PCA-LS-0.5 membranes were characterized by SEM. Fig. 4a and b exhibit the existence of numerous pores on the surface of PES membrane. However, the pore size of PES-PCA-LS-0.5 membrane was much smaller. Compared to these side profiles, a thin layer on PES-PCA-LS-0.5 membrane was about 50 nm and compact compared to that on PES membrane, as shown in Fig. 4c and d. Besides, the space core in the PES membrane decreased after modification, which indicates that its inside was also modified by PCA-LS in the reaction process. Fig. 4e exhibits that the pore size of PES membrane was mainly distributed in the range of 35–50 nm. However, the pore size of all the five modified membranes was reduced from 35–50 nm to 25–45 nm. At the same time, the micropores below 2 nm decreased in number after modification. Interestingly, the average pore size

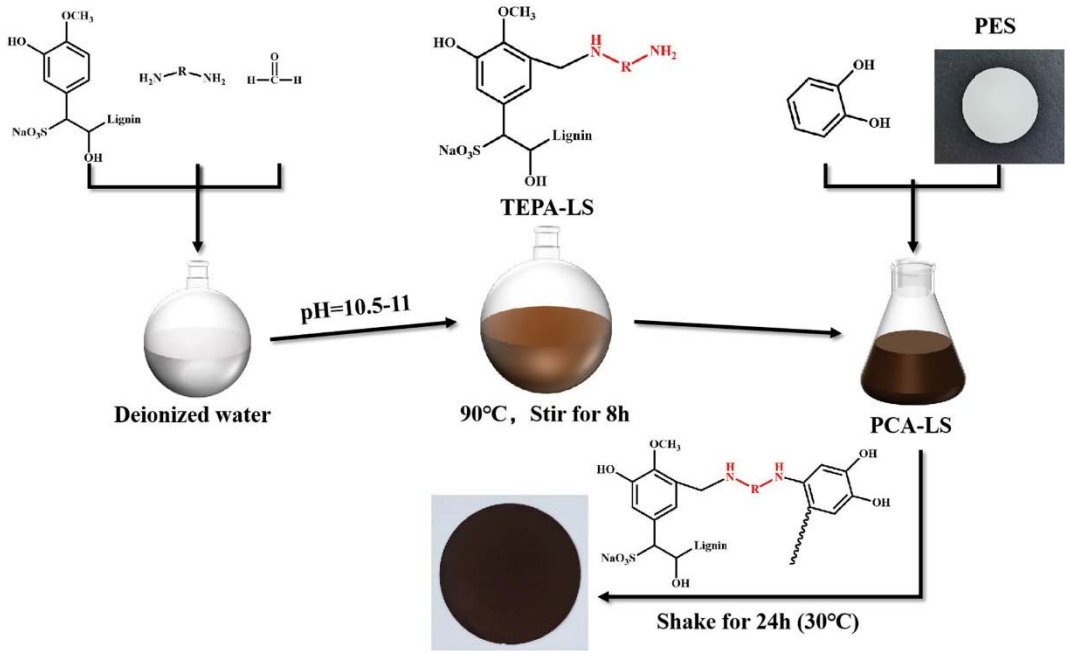

Fig. 2. Schematic representation of the preparation process of PES-PCA-LS membrane.

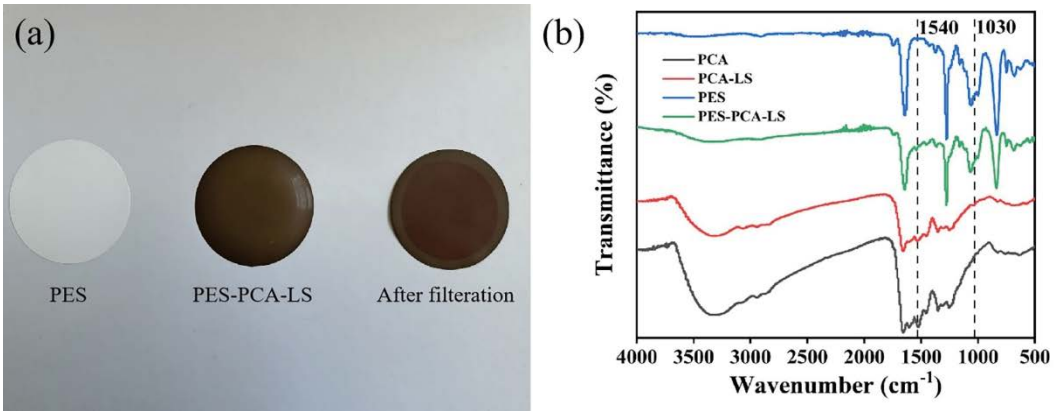

Fig. 3. (a) Photographs of PES and PES-PCA-LS-0.5 membranes before and after filtration, (b) infrared spectral analysis of PCA, PCA-LS, PES, and PES-PCA-LS-0.5 membrane.

of the modified membranes was found to be increased. This may be attributed to the deposition of PCA-LS, resulting in the partial filling of micropores to form larger mesopores. Besides, Fig. 5a and c show that the surface roughness of PES-PCA-LS-0.5 membrane changed significantly after modification. The rough surface of PES membrane provided a larger area for PCA-LS.

deposition. Moreover, PCA-LS was observed to be deposited in these gullies, filling them partially. Fig. 5b and d illustrate that compared with PES membrane, PES-PCA-LS-0.5 membrane was smoother. The average roughness (R_a) decreased from 251 to 104 nm. This was mainly due to the deposited PCA-LS filling up the grooves present on the surface of PES membrane. Based on these characterizations, it was speculated that the surface modification of PES membrane could be accomplished by relying on the adhesion property of PCA-LS, and this modification was not just present on the surface of PES membrane. The deposited PES-PCA-LS-0.5 membrane could decrease the flux by compacting surface and narrowing channel, and thus the separation performance increased due to its adsorption.

3.2. Effect of mass ratios of LS to TEPA on flux and performance

Under the optimized conditions (room temperature, CR concentration of 100 ppm, and NaCl concentration of 5,000 ppm), the performance and fluxes of the PES and five products with different amounts of added LS were tested, separately. The experimental results are shown in Fig. 6a. It was found that the added content of LS played a decisive role in the performance of PES-PCA-LS membrane.

The performance of PES membrane was about 0 L·m^{-2}, which could be ascribed to the definition of performance, according to which the effective removal rate was more than 99.5%. Besides, PES membrane does not contain any functional groups to adsorb CR.

With the increase in the mass ratio of LS to TEPA from 0 to 1:1, the flux first decreased and then increased, and the performance reversed. When the mass ratio of LS to TEPA was 0.5:1, the optimum ratio was reached. The flux and performance of PES-PCA-LS-0 membrane, which was deposited by catechol and TEPA directly, was better than that of PES membrane. Interestingly, the flux increased slightly because the hydrophilicity of the PES-PCA-LS-0 membrane was significantly better than that of PES membrane, and the channel did not become too small to pass through. The increased performance (more than 200 L·m^{-2}) indicates that the deposited PCA plays an important role in rejecting CR.

The flux of PES-PCA-LS-0.25 membrane is less than that of PES-PCA-LS-0 membrane. By testing the membrane mass before and after deposition, the difference quality is the deposition quality of PCA-LS. Fig. 6b demonstrates that the adsorbent deposition on PES-PCA-LS-0.25 membrane was significantly higher than that on PES-PCA-LS-0 membrane due to the addition of LS, which made the channels thinner. The performance of PES-PCA-LS-0.25 membrane was better than that of PES-PCA-LS-0 membrane, revealing that more absorbent was deposited on the composite membrane to remove CR. This also verifies the cross-linking of LS in the PCA, and plays an important role in adsorption. The flux of PES-PCA-LS-0.5 membrane decreases further and the performance increases, which can be attributed to the same reasons.

Compared to that of PES-PCA-LS-0.5 membrane, the flux of PES-PCA-LS-0.75 and PES-PCA-LS-1 membrane increased and the performance decreased, according to the results presented in Fig. 6a. This may be mainly due to the excess of LS. The mass ratio of LS to TEPA decides the number of primary amine groups present in TEPA-LS. The excessive amount of LS may prevent it from reacting with TEPA or the TEPA-LS contains less than two primary amine groups. Thus, the TEPA-LS containing one primary amine group leads to the decrease in the molecular weight of PCA-LS, which further decreases the content of PCA-LS deposited on PES membrane. Consequently, their flux increases and their performance decreases. In summary, the mass ratio of LS to TEPA plays a decisive role in the performance of the composite membrane. When the mass ratio of LS to TEPA is 0.5:1, the composite membrane exhibits the best performance for dye removal.

3.3. Effect of deposition time on performance

The deposition time is a crucial factor that decides the compactness and the depth of the PCA-LS polymer on the composite membrane. Under the conditions (room

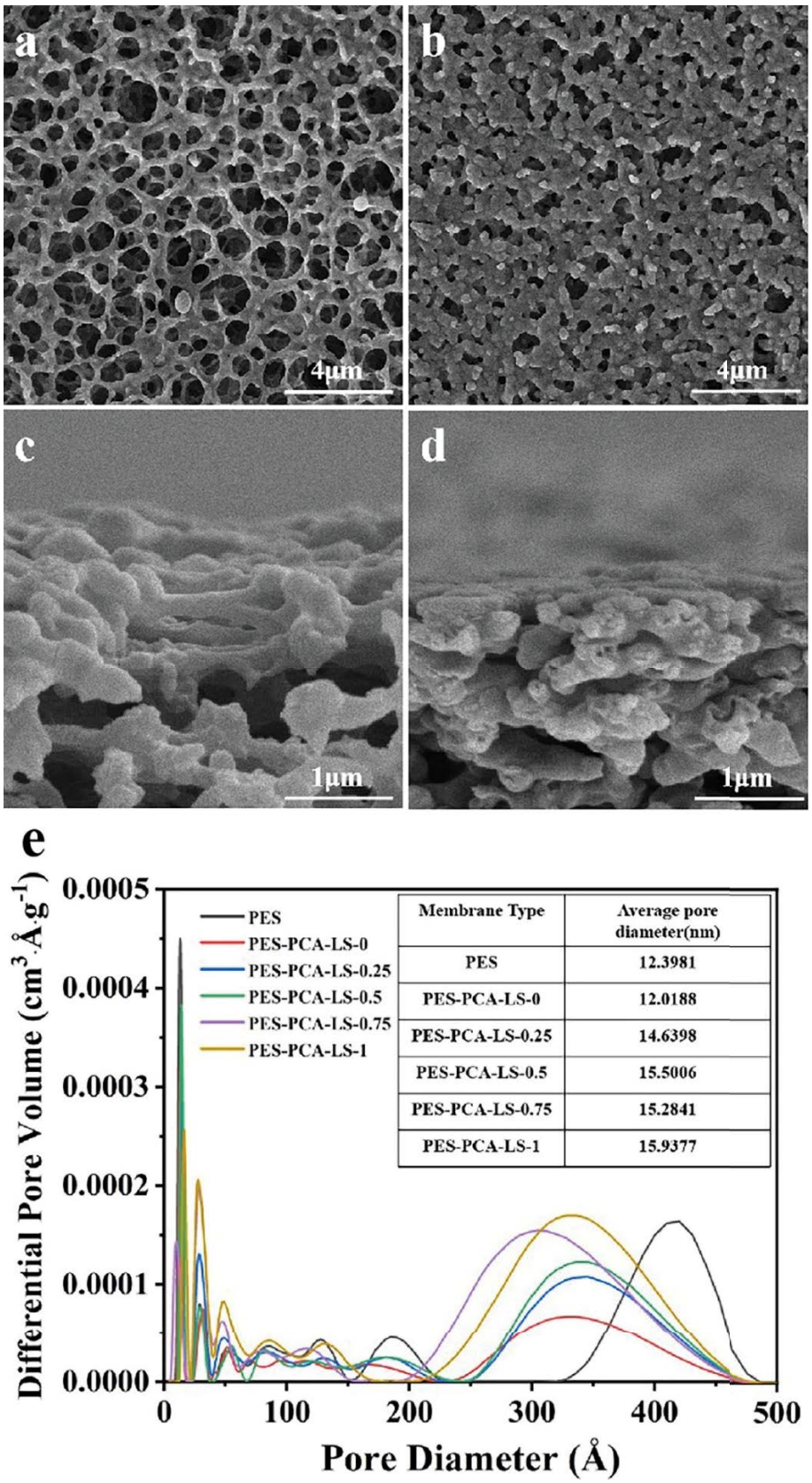

Membrane Type	Average pore diameter(nm)
PES	12.3981
PES-PCA-LS-0	12.0188
PES-PCA-LS-0.25	14.6398
PES-PCA-LS-0.5	15.5006
PES-PCA-LS-0.75	15.2841
PES-PCA-LS-1	15.9377

Fig. 4. SEM images of (a) front surface and (c) side section of PES membrane, SEM images of (b) front surface and (d) side section of PES-PCA-LS membrane, and (e) pore-size distribution of PES and five types of modified membranes.

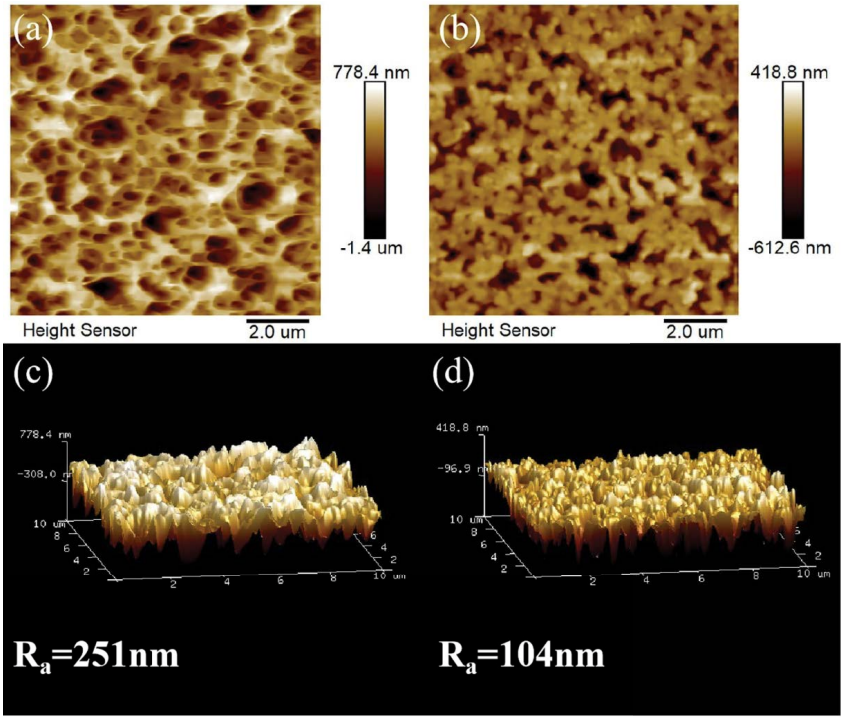

Fig. 5. The 2-dimentional and 3-dimensional AFM images of (a,c) PES membrane and (b,d) PES-PCA-LS-0.5 membrane.

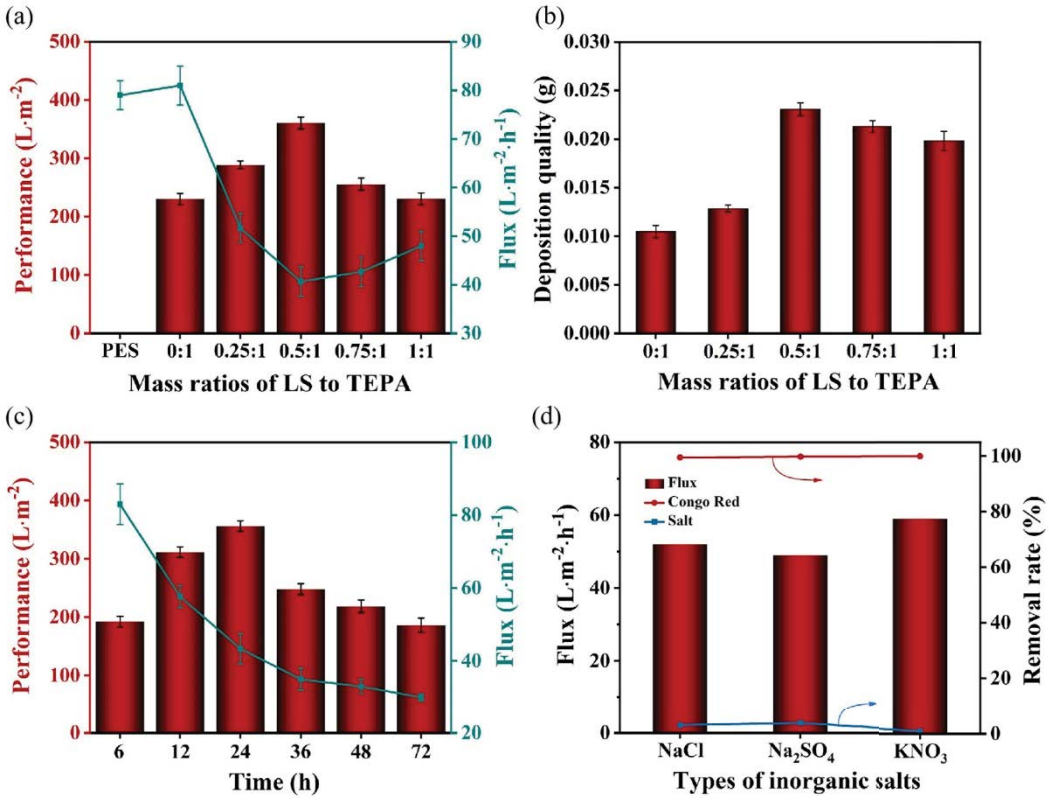

Fig. 6. (a) Effects of mass ratios of LS to TEPA on the performance and flux (room temperature, CR concentration of 100 ppm and NaCl concentration of 5,000 ppm). (b) Effect of LS and TEPA mass ratio on deposition quality. (c) Effects of deposition time on the performance and flux (room temperature, CR concentration of 100 ppm and NaCl concentration of 5,000 ppm). (d) Flux and rejection rate of inorganic salt (room temperature, CR concentration of 100 ppm, inorganic salt concentration of 5,000 ppm).

temperature, CR concentration of 100 ppm, and NaCl concentration of 5,000 ppm), PES-PCA-LS-0.5 membrane was used to investigate the effect of deposition time on performance. Fig. 6c illustrates that the flux decreases continuously with increasing deposition time from 6 to 72 h. It indicates that the channel becomes thinner with the prolonged time. This is mainly because the amount of PCA-LS deposited on the surface and inside PES membrane increases with prolongation of reaction time. The performance first increases and then decreases, reaching the optimum at the deposition time of 24 h. After 24 h, PCA-LS continued to deposit on the membrane, and the channel of PES-PCA-LS-0.5 membrane continued to become smaller. The effective contact area of PCA-LS with the dye becomes smaller. This is the main reason for the performance degradation. In summary, the deposition amount continues to increase with increasing deposition time, but if the deposition amount is higher, the performance of dye removal may not be better. The optimal performance was attained at a deposition time of 24 h.

3.4. Dye/salt separation performance of PES-PCA-LS membrane

In order to further investigate the separation performance of PES-PCA-LS-0.5 membranes for dyes and inorganic salts, the mixtures (100 ppm for CR and 5,000 ppm for salts) of CR and inorganic salt (NaCl, Na_2SO_4, and K_2SO_4, separately) were measured. Fig. 6d exhibits that the PES-PCA-LS-0.5 membrane consistently maintained high retention of the dye, while the rejection rate of NaCl, Na_2SO_4, and K_2SO_4 was 2.8%, 3.5%, and 0.9%, respectively. Analysis of the BET results indicates that the low retention of salt by PES-PCA-LS-0.5 membrane is mainly due to its larger average pore diameter than that of salt. The high retention rate for dyes is mainly attributed to the electrostatic effect of sulfonic acid group and amine group. Besides, the flux did not decrease under high salt concentration conditions while having excellent dye/salt separation performance. In summary, PES-PCA-LS-0.5 membrane exhibits the potential to remove anionic dyes at higher inorganic salt concentrations.

3.5. Adsorption mechanism

It is well known that hydrophilicity is a very important index in evaluating aqueous filter membranes. Fig. 7a demonstrates that the contact angle of PES membrane becomes smaller with the prolongation of time, and reaches about 75° after 5 s. In contrast, the contact angle of PES-PCA-LS-0.5 membrane could reach 50° within 0.5 s, and the value could reach about 10° after 5 s. This may be attributed to the fact that the deposited PES-PCA-LS-0.5 contains more hydrophilic groups (–SO_3–, –OH, –NH–, etc.) on the surface and inside of PES-PCA-LS-0.5 membrane compared to PES membrane.

Fig. 6a exhibits the comparative analysis of the filtration effect of PES and PES-PCA-LS-0.5 membrane on CR, and the average pore size becomes larger after deposition. In dye filtration experiments, the retention rate decreases with the increase in the filtration volume. The above-mentioned results indicate that the retention mechanism of PES-PCA-LS-0.5 membrane is mainly adsorption rather than pore size sieving. To further investigate the adsorption mechanism, the zeta potentials of PES membrane and PES-PCA-LS-0.5 membrane were analyzed. Fig. 7b exhibits that PES membrane is negatively charged in the pH range of 3–10. However, PES-PCA-LS-0.5 membrane presents positive charge in the pH range of 3–8, which is mainly attributed to the large number of amine groups contained in PES-PCA-LS-0.5 membrane. The CR molecule, containing two amine groups and two sulfonic acid groups, is an anionic dye. When the pH of the dye solution is 6.0–6.5, PES-PCA-LS-0.5 membrane can adsorb CR by intermolecular electrostatic interaction. Fig. 8b shows that this conclusion was also confirmed by performing different dye filtration experiments.

Besides, the aromatic ring in the CR molecule can interact with the benzyl ring in PES-PCA-LS-0.5 membrane through π–π stacking. In summary, the retention of anionic dyes by PES-PCA-LS-0.5 membrane is mainly due to the strong electrostatic attraction between the positive charges carried by the amine and sulfonic acid groups and the anionic dye molecules under acidic conditions. The action of electrostatic force is more precise for dye retention by adsorption compared to pore size sieving. Based on this adsorption mechanism, PES-PCA-LS-0.5 membrane exhibits the promising potential for selective retention of dyes.

3.6. Selective filtration of different dyes

The removal rate was measured by filtering 100 mL of solution of different types of dyes (100 ppm) through

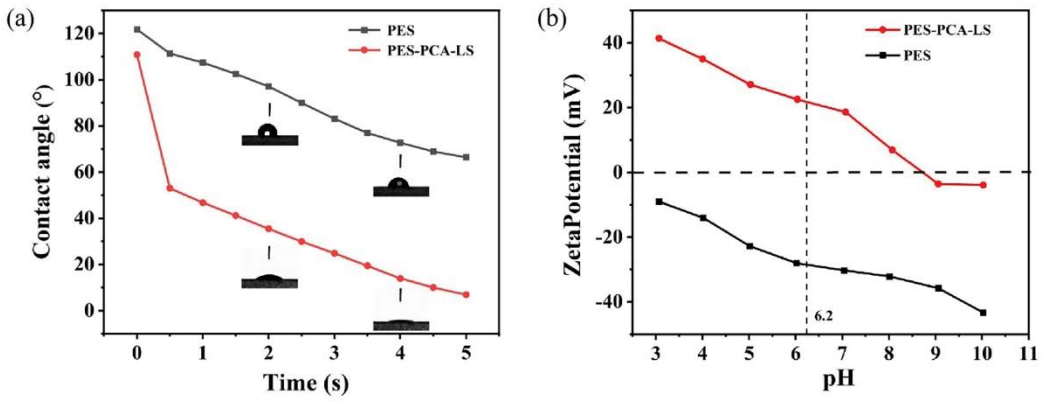

Fig. 7. (a) Water contact angle and (b) zeta potential analysis of PES and PES-PCA-LS membranes.

a PES-PCA-LS-0.5 membrane with an effective area of 12.56 cm^2. Fig. 8a and b exhibit that the removal rates of anionic dyes (CR, MB) are more than 95% and those of cationic dyes (MG, RB) are about 20%. This result further confirms the important role of the electrostatic interaction. It was also found that the removal percentage of MB was less than that of CR due to the specific structure of MB; that is, the secondary amine and the ortho-position between amine and sulphonate groups.

The separation performance of this PES-PCA-LS-0.5 membrane was tested by using CR (anionic dye) and RB (cationic dye) as probes. The mixture (400 mL) of CR (50 ppm) and RB (50 ppm) was filtered and the filtrate was detected by UV spectroscopy. Fig. 8c exhibits that the spectrum of mixture covers the curve of CR and the curve of RB. After filtration, the characteristic peak representing CR at 488 nm almost completely disappears, the spectrum after filtration of mixture is consistent with the curve of RB. Thus, PES-PCA-LS-0.5 membrane may separate CR from its mixture with cationic dyes. In summary, based on the strong electrostatic interaction between PES-PCA-LS-0.5 membrane and anionic dyes, PES-PCA-LS-0.5 membrane attains the potential to selectively retain anionic dyes from the dye mixture.

3.7. Cycle performance and antifouling ability

Cycling performance is important for the utilization of PES-PCA-LS-0.5 membrane. The flux and removal rate were measured by filtering 400 mL of mixed solution of CR (NaCl 5,000 ppm, CR 100 ppm) per cycle through PES-PCA-LS-0.5 membrane with an effective area of 12.56 cm^2. This membrane was desorbed by NaOH solution (pH = 11) to regenerate. Fig. 9a illustrates that the PES-PCA-LS-0.5 membrane after filtration on the left shows a distinct red disc in the middle effective area. After desorption, the red disc is almost completely cleared.

The cycling performance of PES-PCA-LS-0. membrane is shown in Fig. 9b. During the first four cycles, the flux showed a decreasing trend, which was mainly due to the difficulty of washing the adsorbed dye layer thoroughly during the regeneration process, resulting in the accumulation of dye and a gradual decrease in flux. After the fifth cycle, the flux of CR solution filtered with PES-PCA-LS-0.5 membrane remained stable at about 22 $L \cdot m^{-2} \cdot h^{-1}$, while the removal rate decreased gradually and remained 97% at the tenth cycle. This may prove that the PES-PCA-LS-0.5 membrane shows excellent cycling performance.

In order to study the antifouling ability of PES-PCA-LS-0.5 membrane during cycling, the FRR, R_r, and R_{ir} of PES and PES-PCA-LS-0.5 membrane were studied after ten cycles. Table 1 presents that the FRR of PES-PCA-LS-0.5 membrane was lower than that of PES membrane by about thirteen percentage points after ten cycles. This is mainly due to the fact that PES-PCA-LS-0.5 membrane channel is smaller and more prone to clogging than PES membrane channel. Compared to those of PES membrane, both R_r and

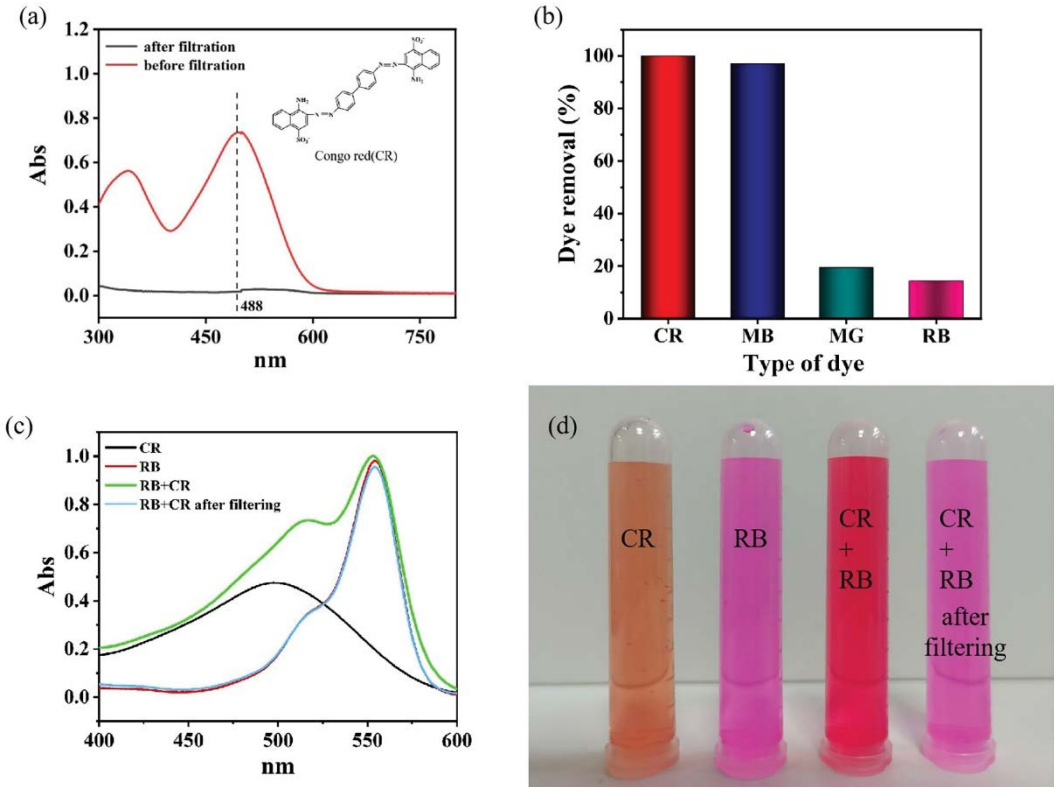

Fig. 8. (a) UV-Vis absorption spectra of CR solution before (red) and after (black) filtration, (b) filtration test of cationic (MG, RB) and anionic (CR, MB) dyes, (c) separation of CR from its mixture with RB, and (d) photographs of selective filtering of CR from RB/CR mixture.

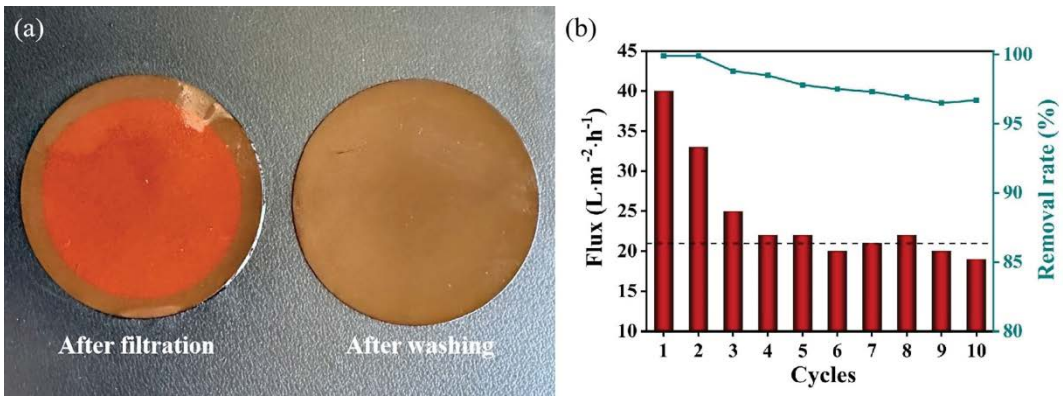

Fig. 9. (a) Photographs of PES-PCA-LS-0.5 membrane after filtration and after washing and (b) cyclic performance of PES-PCA-LS-0.5 membrane.

Table 1
FRR, R_r, R_{ir} of the pristine PES and PES-PCA-LS-0.5 membranes

Number of cycles	PES			PES-PCA-LS-0.5		
	FRR	R_r	R_{ir}	FRR	R_r	R_{ir}
10th	89%	7%	10%	76%	15%	23%

R_{ir} of PES-PCA-LS-0.5 membrane were almost twice, because it was not possible to completely desorb the adsorbed CR during the adsorption and desorption processes. This could lead to partial blockage of the channels. This finding also confirms the reason why the flux decrease is mainly concentrated in the first four cycles, as shown in Fig. 9b. In summary, although the antifouling capacity decreases after modification, it is within the acceptable range. However, the significant improvement in separation of CR was obtained after the modification is more important.

4. Conclusion

In this study, PES-PCA-LS membranes were prepared by a simple deposition method. Various characterizations of PES-PCA-LS membrane confirmed the successful modification of PES membrane, leading to smoother surface and better hydrophilicity of PES-PCA-LS membrane. With a CR removal rate of 99.5%, each m^2 of PES-PCA-LS membrane could treat approximately 350 L of a mixture of CR and salt (CR, 100 ppm; NaCl, 5,000 ppm). Simultaneously, it maintained low retention of inorganic salts (NaCl, 2.8%; Na_2SO_4, 3.5%; K_2SO_4, 0.9%). PES-PCA-LS membrane showed excellent selectivity for anionic dyes in filtration experiments on mixed dyes. It was able to retain anionic dyes from a mixture of anionic and cationic dyes. Dye separation experiments were conducted on PES-PCA-LS membrane containing different amounts of added sodium lignosulfonate to optimize the amount of sodium lignosulfonate. The recycling and antifouling experiments illustrated that the antifouling performance was slightly reduced after modification. However, the separation performance of PES-PCA-LS membrane for dyestuffs decreased by less than 2% in cycling. Thus, PES-PCA-LS membrane did not lose too much flux and antifouling performance compared to the unmodified PES membrane. At the same time, excellent dye separation performance and circulation performance were obtained. This makes PES-PCA-LS membrane a promising candidate in the field of dye wastewater treatment.

Abbreviations

PES, polyethersulfone. PES-PCA-LS, lignosulfonate-based polycatecholamine and polyethersulfone composite. PCA-LS, lignosulfonate-based polycatecholamine. MB, Methyl blue. RB, Rhodamine B. CR, Congo red. MG, Malachite green. LS, sodium lignosulfonate. TEPA, tetraethylenepentamine. TEPA-LS, the product obtained by Mannich reaction of sodium lignosulfonate, formaldehyde, and tetraethylenepentamine. PCA, products obtained from the reaction of tetraethylenepentamine with catechol. FRR, flux recovery ratio. R_r, flux decline ratio due to reversible fouling effects. R_{ir}, flux decline ratio due to irreversible fouling effects. Performance, the maximum volume of Congo red waste solution that could be treated per square meter with a 99.5% removal rate.

Acknowledgements

This work was supported by Natural Science Foundation of Shandong Province [ZR2020ME072, ZR2020ME082]; Youth Innovation Team Development Plan of Universities in Shandong Province (Grant No. 2021KJ056) and the Universities Twenty Foundational Items of Jinan City [2020GXRC027, 2021GXRC097, 2021GXRC068].

References

[1] E.F.D. Januário, T.B. Vidovix, N. de Camargo Lima Beluci, R.M. Paixão, L.H.B.R. da Silva, N.C. Homem, R. Bergamasco, A.M.S. Vieira, Advanced graphene oxide-based membranes as a potential alternative for dyes removal: a review, Sci. Total Environ., 789 (2021) 147957, doi: 10.1016/j.scitotenv.2021.147957.
[2] X. Liang, P. Wang, J. Wang, Y. Zhang, W. Wu, J. Liu, B. Van der Bruggen, Zwitterionic functionalized MoS_2 nanosheets for a novel composite membrane with effective salt/dye separation performance, J. Membr. Sci., 573 (2019) 270–279.
[3] J.H. Shin, J.E. Yang, J.E. Park, S.W. Jeong, S.J. Choi, Y.J. Choi, J. Jeon, Rapid and efficient removal of anionic dye in water

using a chitosan-coated iron oxide-immobilized polyvinylidene fluoride membrane, ACS Omega, 7 (2022) 8759–8766.
[4] X. Feng, D. Peng, J. Zhu, Y. Wang, Y. Zhang, Recent advances of loose nanofiltration membranes for dye/salt separation, Sep. Purif. Technol., 285 (2022) 120228, doi: 10.1016/j.seppur.2021.120228.
[5] H. Nawaz, M. Umar, A. Ullah, H. Razzaq, K.M. Zia, X. Liu, Polyvinylidene fluoride nanocomposite super hydrophilic membrane integrated with polyaniline-graphene oxide nano fillers for treatment of textile effluents, J. Hazard. Mater., 403 (2021) 123587, doi: 10.1016/j.jhazmat.2020.123587.
[6] T. Puspasari, K.-V. Peinemann, Application of thin film cellulose composite membrane for dye wastewater reuse, J. Water Process Eng., 13 (2016) 176–182.
[7] A.J. Sutherland, M.-X. Ruiz-Caldas, C.-F. de Lannoy, Electrocatalytic microfiltration membranes electrochemically degrade azo dyes in solution, J. Membr. Sci., 611 (2020) 118335, doi: 10.1016/j.memsci.2020.118335.
[8] X.-l. Wang, W. Qin, L.-x. Wang, K.-y. Zhao, H.-c. Wang, H.-y. Liu, J.-f. Wei, Desalination of dye utilizing carboxylated TiO_2/calcium alginate hydrogel nanofiltration membrane with high salt permeation, Sep. Purif. Technol., 253 (2020) 117475, doi: 10.1016/j.seppur.2020.117475.
[9] S. Benkhaya, H. Lgaz, S. Chraibi, A.A. Alrashdi, M. Rafik, H.-S. Lee, A. El Harfi, Polysulfone/Polyetherimide Ultrafiltration composite membranes constructed on a three-component Nylon-fiberglass-Nylon support for azo dyes removal: experimental and molecular dynamics simulations, Colloids Surf., A, 625 (2021) 126941, doi: 10.1016/j.colsurfa.2021.126941.
[10] W. Chen, J. Mo, X. Du, Z. Zhang, W. Zhang, Biomimetic dynamic membrane for aquatic dye removal, Water Res., 151 (2019) 243–251.
[11] F. Sheng, X. Li, Y. Li, N.U. Afsar, Z. Zhao, L. Ge, T. Xu, Cationic covalent organic framework membranes for efficient dye/salt separation, J. Membr. Sci., 644 (2022) 126941, doi: 10.1016/j.memsci.2021.120118.
[12] C. Cojocaru, L. Clima, Polymer assisted ultrafiltration of AO7 anionic dye from aqueous solutions: experimental design, multivariate optimization, and molecular docking insights, J. Membr. Sci., 604 (2020) 118054, doi: 10.1016/j.memsci.2020.118054.
[13] S. Masoudnia, M.H. Juybari, R.Z. Mehrabian, M. Ebadi, F. Kaveh, Efficient dye removal from wastewater by functionalized macromolecule chitosan-SBA-15 nanofibers for biological approaches, Int. J. Biol. Macromol., 165 (2020) 118–130.
[14] V. Vatanpour, N. Haghighat, Improvement of polyvinyl chloride nanofiltration membranes by incorporation of multiwalled carbon nanotubes modified with triethylenetetramine to use in treatment of dye wastewater, J. Environ. Manage., 242 (2019) 90–97.
[15] S. Yi, S. Sun, Y. Zhang, Y. Zou, F. Dai, Y. Si, Scalable fabrication of bimetal modified polyacrylonitrile (PAN) nanofibrous membranes for photocatalytic degradation of dyes, J. Colloid Interface Sci., 559 (2020) 134–142.
[16] Z. Huang, J. Liu, Y. Liu, Y. Xu, R. Li, H. Hong, L. Shen, H. Lin, B.-Q. Liao, Enhanced permeability and antifouling performance of polyether sulfone (PES) membrane via elevating magnetic Ni@MXene nanoparticles to upper layer in phase inversion process, J. Membr. Sci., 623 (2021) 119080, doi: 10.1016/j.memsci.2021.119080.
[17] Y. Xiao, W. Zhang, Y. Jiao, Y. Xu, H. Lin, Metal-phenolic network as precursor for fabrication of metal-organic framework (MOF) nanofiltration membrane for efficient desalination, J. Membr. Sci., 624 (2021) 119101, doi: 10.1016/j.memsci.2021.119101.
[18] A. Avornyo, A. Thanigaivelan, R. Krishnamoorthy, S.W. Hassan, F. Banat, Ag-CuO-decorated ceramic membranes for effective treatment of oily wastewater, Membranes (Basel), 13 (2023) 176, doi: 10.3390/membranes13020176.
[19] T. Arumugham, M. Ouda, R. Krishnamoorthy, A. Hai, N. Gnanasundaram, S.W. Hasan, F. Banat, Surface-engineered polyethersulfone membranes with inherent Fe-Mn bimetallic oxides for improved permeability and antifouling capability, Environ. Res., 204 (2022) 112390, doi: 10.1016/j.envres.2021.112390.
[20] M. Ouda, Y. Ibrahim, F. Banat, S.W. Hasan, Oily wastewater treatment via phase-inverted polyethersulfone-maghemite (PES/γ-Fe_2O_3) composite membranes, J. Water Process Eng., 37 (2020) 101545, doi: 10.1016/j.jwpe.2020.101545.
[21] J. Lv, G. Zhang, H. Zhang, C. Zhao, F. Yang, Improvement of antifouling performances for modified PVDF ultrafiltration membrane with hydrophilic cellulose nanocrystal, Appl. Surf. Sci., 440 (2018) 1091–1100.
[22] C. Shen, L. Bian, P. Zhang, B. An, Z. Cui, H. Wang, J. Li, Microstructure evolution of bonded water layer and morphology of grafting membrane with different polyethylene glycol length and their influence on permeability and anti-fouling capacity, J. Membr. Sci., 601 (2020) 117949, doi: 10.1016/j.memsci.2020.117949.
[23] Y. Liu, Z. Huang, Z. Zhang, X. Lin, Q. Li, Y. Zhu, A high stability GO nanofiltration membrane preparation by co-deposition and crosslinking polydopamine for rejecting dyes, Water Sci. Technol., 85 (2022) 1783–1799.
[24] P. Ge, Z. Lin, J. Yang, C. Hu, Q. Liu, Q. Zhang, Polyethylenimine grafted hollow fiber membranes for fast dye separation, J. Membr. Sci., 672 (2023) 121428, doi: 10.1016/j.memsci.2023.121428.
[25] X. Yang, Y. Zhou, Z. Sun, C. Yang, D. Tang, Synthesis and Cr adsorption of a super-hydrophilic polydopamine-functionalized electrospun polyacrylonitrile, Environ. Chem. Lett., 19 (2020) 743–749.
[26] S. Devadas, S.M.N. Al-Ajrash, D.A. Klosterman, K.M. Crosson, G.S. Crosson, E.S. Vasquez, Fabrication and characterization of electrospun poly(acrylonitrile-co-methyl acrylate)/lignin nanofibers: effects of lignin type and total polymer concentration, Polymers (Basel), 13 (2021) 992, doi: 10.3390/polym13070992.
[27] R.J. Beck, Y. Zhao, H. Fong, T.J. Menkhaus, Electrospun lignin carbon nanofiber membranes with large pores for highly efficient adsorptive water treatment applications, J. Water Process Eng., 16 (2017) 240–248.
[28] J. Fang, Y. Chen, C. Fang, L. Zhu, Regenerable adsorptive membranes prepared by mussel-inspired co-deposition for aqueous dye removal, Sep. Purif. Technol., 281 (2022) 119876, doi: 10.1016/j.seppur.2021.119876.
[29] Q. Li, Z. Liao, X. Fang, D. Wang, J. Xie, X. Sun, L. Wang, J. Li, Tannic acid-polyethyleneimine crosslinked loose nanofiltration membrane for dye/salt mixture separation, J. Membr. Sci., 584 (2019) 324–332.
[30] W. Ye, K. Ye, F. Lin, H. Liu, M. Jiang, J. Wang, R. Liu, J. Lin, Enhanced fractionation of dye/salt mixtures by tight ultrafiltration membranes via fast bio-inspired co-deposition for sustainable textile wastewater management, Chem. Eng. J., 379 (2020) 122321, doi: 10.1016/j.cej.2019.122321.
[31] G. Zeng, Z. Ye, Y. He, X. Yang, J. Ma, H. Shi, Z. Feng, Application of dopamine-modified halloysite nanotubes/PVDF blend membranes for direct dyes removal from wastewater, Chem. Eng. J., 323 (2017) 572–583.
[32] J. Zhao, Y. Su, X. He, X. Zhao, Y. Li, R. Zhang, Z. Jiang, Dopamine composite nanofiltration membranes prepared by self-polymerization and interfacial polymerization, J. Membr. Sci., 465 (2014) 41–48.
[33] Y. Chen, C. He, High salt permeation nanofiltration membranes based on NMG-assisted polydopamine coating for dye/salt fractionation, Desalination, 413 (2017) 29–39.
[34] D. Guo, Y. Xiao, T. Li, Q. Zhou, L. Shen, R. Li, Y. Xu, H. Lin, Fabrication of high-performance composite nanofiltration membranes for dye wastewater treatment: mussel-inspired layer-by-layer self-assembly, J. Colloid Interface Sci., 560 (2020) 273–283.
[35] L. Jin, Y. Gao, J. Yin, X. Zhang, C. He, Q. Wei, X. Liu, F. Liang, W. Zhao, C. Zhao, Functionalized polyurethane sponge based on dopamine derivative for facile and instantaneous clean-up of cationic dyes in a large scale, J. Hazard. Mater., 400 (2020) 123203, doi: 10.1016/j.jhazmat.2020.123203.

[36] Y. Zhan, X. Wan, S. He, Q. Yang, Y. He, Design of durable and efficient poly(arylene ether nitrile)/bioinspired polydopamine coated graphene oxide nanofibrous composite membrane for anionic dyes separation, Chem. Eng. J., 333 (2018) 132–145.
[37] J. Wang, R. He, X. Han, D. Jiao, J. Zhu, F. Lai, X. Liu, J. Liu, Y. Zhang, B. Van der Bruggen, High performance loose nanofiltration membranes obtained by a catechol-based route for efficient dye/salt separation, Chem. Eng. J., 375 (2019) 121982, doi: 10.1016/j.cej.2019.121982.
[38] H.C. Yang, R.Z. Waldman, M.B. Wu, J. Hou, L. Chen, S.B. Darling, Z.K. Xu, Dopamine: just the right medicine for membranes, Adv. Funct. Mater., 28 (2018) 1705327, doi: 10.1002/adfm.201705327.
[39] H.-C. Yang, M.-B. Wu, Y.-J. Li, Y.-F. Chen, L.-S. Wan, Z.-K. Xu, Effects of polyethyleneimine molecular weight and proportion on the membrane hydrophilization by codepositing with dopamine, J. Appl. Polym. Sci., 133 (2016) 43729, doi: 10.1002/app.43792.
[40] X. Zhang, C. Liu, J. Yang, X.-J. Huang, Z.-K. Xu, Wettability switchable membranes for separating both oil-in-water and water-in-oil emulsions, J. Membr. Sci., 624 (2021) 118976, doi: 10.1016/j.memsci.2020.118976.
[41] L. Xu, X. Yang, H. Ding, S. Li, M. Li, D. Wang, J. Xia, Synthesis of green fluorescent carbon materials using byproducts of the sulfite-pulping procedure residue for live cell imaging and Ag(⁺) ion determination, Mater. Sci. Eng., C, 102 (2019) 917–922.
[42] G. Zhou, T. Fan, Y. Ma, Preparation and chemical characterization of an environmentally-friendly coal dust cementing agent, J. Chem. Technol. Biotechnol., 92 (2017) 2699–2708.
[43] L. Li, B. Dou, J. Lan, J. Shang, Y. Wang, J. Yu, E. Ren, S. Lin, Scalable sulfonate-coated cotton fibers as facile recyclable adsorbents for the highly efficient removal of cationic dyes, Cellulose, 29 (2022) 7445–7463.
[44] R. Luo, W. Zhang, X. Hu, Y. Liang, J. Fu, M. Liu, F. Deng, Q.-Y. Cao, X. Zhang, Y. Wei, Preparation of sodium ligninsulfonate functionalized MXene using hexachlorocyclotriphosphazene as linkage and its adsorption applications, Appl. Surf. Sci., 602 (2022) 154197, doi: 10.1016/j.apsusc.2022.154197.
[45] C. Wang, J. Zhang, C. Liu, X. Song, C. Zhang, Wood–inspired preparation of ligninsulfonate/trimesoylchloride nanofilm with a highly negatively charged surface for removing anionic dyes, Chem. Eng. J., 412 (2021) 128609, doi: 10.1016/j.cej.2021.128609.
[46] A. Xie, J. Dai, Y. Chen, N. Liu, W. Ge, P. Ma, R. Zhang, Z. Zhou, S. Tian, C. Li, Y. Yan, NaCl-template assisted preparation of porous carbon nanosheets started from lignin for efficient removal of tetracycline, Adv. Powder Technol., 30 (2019) 170–179.
[47] L. Xu, W. Mao, J. Huang, S. Li, K. Huang, M. Li, J. Xia, Q. Chen, Economical, green route to highly fluorescence intensity carbon materials based on ligninsulfonate/graphene quantum dots composites: application as excellent fluorescent sensing platform for detection of Fe^{3+} ions, Sens. Actuators, B, 230 (2016) 54–60.
[48] S. Gao, G. Wei, Q. Liu, Q. Liu, T. Gao, J. Yao, Efficient removal of Congo red from pH-unregulated aqueous solutions by lignosulfonate-based polycatecholamine, J. Appl. Polym. Sci., 137 (2019) 48640, doi: 10.1002/app.48640.
[49] M. Ouda, A. Hai, R. Krishnamoorthy, B. Govindan, I. Othman, C.C. Kui, M.Y. Choi, S.W. Hasan, F. Banat, Surface tuned polyethersulfone membrane using an iron oxide functionalized halloysite nanocomposite for enhanced humic acid removal, Environ. Res., 204 (2022) 112113, doi: 10.1016/j.envres.2021.112113.